Hot-Electron Degradation of AlGaN/GaN High-Electron Mobility Transistors During RF Operation: Correlation With GaN Buffer Design

Davide Bisi, Alessandro Chini, Fabio Soci, Antonio Stocco, Matteo Meneghini, *Senior Member, IEEE*, Alessio Pantellini, Antonio Nanni, Claudio Lanzieri, Piero Gamarra, Cedric Lacam, Maurice Tordjman, Marie-Antoinette di-Forte-Poisson, Gaudenzio Meneghesso, *Fellow, IEEE*, and Enrico Zanoni, *Fellow, IEEE*

Abstract—Comprehensive RF stress-test campaign has been performed over AlGaN/GaN high-electron mobility transistor employing different GaN buffer designs, including unintentional doping, carbon doping and iron doping. No signature of gate-edge degradation has been found, and good correlation emerges between the buffer composition, subthreshold leakage current, and permanent degradation of the RF performance. The degradation mechanism, more pronounced in devices with parasitic buffer conductivity, involves the generation of additional deep trap states, the worsening of the dynamic current collapse, and the subsequent degradation of RF output power.

Index Terms—GaN, HEMT, RF, degradation, current collapse, buffer compensation.

INTRODUCTION

Long-term reliability of GaN-based HEMTs (High Electron Mobility Transistors) is a key aspect for the successful integration of the promising GaN-based electronics in high-power microwave applications. During RF operation, GaN HEMTs are subjected to the most stressful conditions, involving high current density, high electric fields and high channel temperature. Consequently, reliability evaluation should include RF accelerated testing as an essential part: RF operation can indeed induce failure modes and mechanisms that are not observed during DC or thermal storage tests [1].

Among the key technological aspects of GaN HEMTs, the compensation of the unintentional n-type conductivity of the GaN buffer layers (e.g., by means of iron or carbon doping) is of essential importance for the optimization of the 2DEG carrier confinement, the substrate insulation, and the control of the short-channel effects [2]–[4]. With this letter, we present an analysis of the relevant interplay between compensation strategy, pinch-off properties, and degradation mechanisms in RF-tested AlGaN/GaN HEMTs.

Results can be summarized as follows: (i) degradation consists of an increase of dynamic current collapse, with consequent degradation of RF performances; no DC degradation is observed; (ii) in particular, the worsening of current collapse effects is caused by an increase of the concentration of two traps with E_A = 0.79 eV and $\sigma_c = 6 \times 10^{-13}$ cm^2 and E_A = 0.84 eV, $\sigma_c = 4 \times 10^{-14}$ cm^2, detected in unintentionally doped (u.i.d.) and 10^{17} cm^{-3} C-doped buffer devices; finally (iii) a good correlation has been found between the subthreshold leakage current in untreated devices and the amount of RF power degradation under RF operation, thus suggesting an enhancement of hot-electron effects during RF operation when the dynamic load line reaches deep pinchoff conditions and the devices with poor carrier confinement do not completely turn off. Since this mechanism is

enhanced by short-channel effects and by poor carrier confinement, it strongly depends on GaN buffer compensation characteristics.

EXPERIMENTAL DETAILS

Devices under test belong to fourteen wafers differing only for GaN buffer design. HEMTs were fabricated using the same process steps and layout, with a 0.5μm Ni/Au gate; they adopted an AlGaN/GaN heterostructure with nominal 25% Al concentration and 23 nm AlGaN thickness, and different buffer compensation, including either no doping (type I), 10^{17} cm^{-3} C-doping (type II), 10^{17} cm^{-3} Fe-doping (type III), or 10^{18} cm^{-3} Fe and 10^{18} cm^{-3} C co-doping (type IV). A PECVD silicon nitride passivation was employed during the process in order to reduce surface leakage and surface-related current collapse. Before starting the RF tests, devices were subjected to load-pull characterization in order to identify optimal matching conditions. Load matching point was chosen as a compromise between maximum output power and PAE. Fresh devices from each wafer were subjected to a 24 h CW RF test at 2.5 GHz with quiescent bias at (V_{DS} = 30 V, I_D = 30% I_{DSS}) and driven into a 6 dB compression point. Base-plate temperature was set to 40°C. The characterization protocol performed prior to and after the stress tests includes static and pulsed I_D-V_D and I_D-V_G measurements and Drain Current Transient Spectroscopy (DCTS) [5].

RESULTS

Devices subjected to 24-hours RF test experienced a degradation on the RF output power (ΔP_{OUT}) ranging from −0.05 dBm to −1.1 dBm. From static measurements performed prior to and after the stress, no worsening of the gate leakage current was detected, even in devices with ΔP_{OUT} = −1 dBm (Figure 1a). This suggests that the gate-edge degradation (e.g. caused by converse piezoelectric effects, time dependent breakdown, or electrochemical GaN oxidation [6]) is not the dominant degradation mechanism. Likewise, no correlation can be found between the degradation of RF performances and the variation of the DC parameters (on average the devices experienced an I_{DSS} decrease of ∼4%, with a Pearson's correlation coefficient $|r|$ of 0.18 with the degradation of the output power). Conversely, the main evidence of device degradation is a significant worsening of the current-collapse. Figure 1b shows the pulsed I_D-V_D characteristics of a representative device with u.i.d. buffer (type I) which experienced a ΔP_{OUT} of −1 dBm. Though no significant degradation is found in the reference quiescent-bias point ($V_{G,Q}$;$V_{D,Q}$) = (0V;0V), a remarkable drain-current degradation (−25% at V_{DS} = 4 V) is found in the hot quiescent bias-point ($V_{G,Q}$;$V_{D,Q}$)= (V_{TH}+0.5V;25V). Figure 2 shows the correlation (with a Pearson's correlation coefficient $|r|$ of 0.77) between the increase of current-collapse and the decrease of RF output power among all tested wafers. By investigating the causes of reported degradation, it has been noticed that the ΔP_{OUT} is more pronounced in those devices that feature worse pinch-off properties and enhanced short-channel effects (Figure 3). Though featuring similar subthreshold-slope and gate leakage-current, devices grown on u.i.d. GaN buffer have higher drain-induced barrier lowering effects (DIBL) higher source-to-drain leakage current ($I_{D,LEAK}$), and experience higher P_{OUT} degradation than devices grown on 10^{18} cm^{-3} Fe and C co-doped buffer. An intermediate behavior is shown by devices employing the other types of buffer, leading to a remarkable correlation ($|r|$ = 0.82) between the ΔP_{OUT} and the initial drain-source leakage (Figure 4a). The source-floating gate-drain breakdown voltages of u.i.d. and 10^{18} cm^{-3} Fe and C co-doped samples are 171V and 155V, respectively. No correlation is found between ΔP_{OUT} and the average power dissipated during the

RF stress (Figure 4b). These results provide an evidence on the correlation between hot-electron degradation mechanisms, already observed in GaN-based HEMTs [7]–[10], and parasitic unintentional conductivity of GaN buffer layers. When devices are driven towards pinch-off, they cross regions of operation characterized by significant current densities and relatively high V_{DS} and electric field magnitude. If parasitic buffer conductivity is present, source-to-drain subthreshold leakage is maintained beyond pinch-off, possibly generating a high density of highly energetic carriers (hot-electrons) which can induce defects in the AlGaN and/or in the GaN

layers, e.g., through the direct damage of weak lattice bonds or the dehydrogenation of Ga vacancies or N antisites complexes [9]. More in details, double-pulsed gm vs V_{GS} characteristics (Figure 5a and Figure 6a) show that the increase of current dispersion after the RF testing is manifested in the drop of the dynamic transconductance (up to 60% in u.i.d. samples) accompanied by no V_{TH} degradation. As reported in [11], the degradation of the dynamic transconductance could be ascribed to the generation of additional trap states localized in the access regions. Thanks to drain current transient spectroscopy (Figure 5b and Figure 6b), it can be noticed that the worsening of current-collapse in u.i.d. and 10^{17} cm^{-3} C-doped buffer devices is caused by an increase of the concentration of the traps with activation energy E_A = 0.79 eV and capture cross-section $\sigma_c = 6 \times 10^{-13}$ cm^2 (labelled E3) and E_A = 0.84 eV, $\sigma_c = 4 \times 10^{-14}$ cm^2 (labelled E4) [12], [13]. On the other hand, though devices with 10^{18} cm^{-3} Fe- and 10^{18} cm^{-3} C co-doping feature higher initial current dispersion (mainly caused by the trap E2, with E_A = 0.56 eV and $\sigma_c = 5 \times 10^{-15}$ cm^2 [14]), they experience negligible decrease of the dynamic transconductance and negligible increase of trap density after RF operations. The Arrhenius plot with the signatures of the detected deep-levels is reported in Figure 7.

CONCLUSION

RF degradation of AlGaN/GaN HEMTs not affected by gate-degradation has been studied. The degradation of the RF output power is correlated with the initial subthreshold leakage current and, consequently, with buffer compensation. In devices with non-optimal buffer compensation, the degradation of the RF output power is caused by the increase of pre-existing defect density, and the worsening of the current collapse. Though featuring higher initial current-collapse, devices with 10^{18} cm^{-3} Fe- and $10^{18}$$cm^{-3}$ C co-doped buffer experience improved subthreshold behavior and more reliable RF operations.

REFERENCES

[1] A. Chini, V. Di Lecce, F. Fantini, G. Meneghesso, and E. Zanoni, “Analysis of GaN HEMT failure mechanisms during DC and large signal RF operation,” *IEEE Trans. Electron Devices*, vol. 59, no. 5, pp. 1385–1392, May 2012. DOI: 10.1109/TED.2012.2188636

[2] M. J. Uren, D. G. Hayes, R. S. Balmer, D. J. Wallis, K. P. Hilton, J. O. Maclean, T. Martin, C. Roff, P. McGovern, J. Benedikt, and P. J. Tasker, “Control of short-channel effects in GaN/AlGaN HFETs,” in *Proc. 1st Eur. Microw. Integr. Circuits Conf.*, Manchester, U.K., Sep. 2006, pp. 65–68. DOI: 10.1109/EMICC.2006.282751

[3] S. Heikman, S. Keller, T. Mates, S. P. DenBaars, and U. K. Mishra, “Growth and characteristics of Fe-doped GaN,” *J. Crystal Growth*, vol. 248, pp. 513–517, Feb. 2003. DOI: 10.1016/S0022-0248(02)01926-7

[4] A. E. Wickenden, D. D. Koleske, R. L. Henry, M. E. Twigg, and M. Fatemi, “Resistivity control in unintentionally doped GaN films grown by MOCVD,” *J. Crystal Growth*, vol. 260, pp. 54–62, Jan. 2004. DOI: 10.1016/j.jcrysgro.2003.08.024

[5] D. Bisi, M. Meneghini, C. De Santi, A. Chini, M. Dammann, P. Bruckner, M. Mikulla, G. Meneghesso, and E. Zanoni, “Deeplevel characterization in GaN HEMTs—Part I: Advantages and limitations of drain current transient measurements,” *IEEE Trans. Electron Devices*, vol. 60, no. 10, pp. 3166–3175, Oct. 2013. DOI: 10.1109/TED.2013.2279021

[6] E. Zanoni, M. Meneghini, A. Chini, D. Marcon, and G. Meneghesso, “AlGaN/GaN-based HEMTs failure physics and reliability: Mechanisms affecting gate edge and Schottky junction,” *IEEE Trans. Electron Devices*, vol. 60, no. 10, pp. 3119–3131, Oct. 2013. DOI: 10.1109/TED.2013.2271954

[7] H. Kim, A. Vertiatchikh, R. M. Thompson, V. Tilak, T. R. Prunty, J. R. Shealy, and L. F. Eastman, “Hot electron induced degradation of undoped AlGaN/GaN HFETs,” *Microelectron. Rel.*, vol. 43, no. 6, pp. 823–827, Jun. 2003. DOI: 10.1016/S0026-2714(03)00066-0

[8] M. Meneghini, A. Stocco, R. Silvestri, G. Meneghesso, and E. Zanoni, “Degradation of AlGaN/GaN high electron mobility transistors related to hot electrons,” *Appl. Phys. Lett.*, vol. 100, pp. 233508-1–233508-3, Jun. 2012. [Online]. Available: http://dx.doi.org/10.1063/1.4723848

[9] Y. Puzyrev, S. Mukherjee, J. Chen, T. Roy, M. Silvestri, R. D. Schrimpf, D. M. Fleetwood, J. Singh, J. M. Hinckley, A. Paccagnella, and S. T. Pantelides, “Gate bias dependence of defect-mediated hot-carrier degradation in GaN HEMTs,” *IEEE Trans. Electron Devices*, vol. 61, no. 5, pp. 1316–1320, May 2014. DOI: 10.1109/TED.2014.2309278

[10] M. Tapajna, N. Killat, V. Palankovski, D. Gregusova, K. Cico, J.-F. Carlin, N. Grandjean, M. Kuball, and J. Kuzmik, “Hot-electron related degradation in InAlN/GaN high-electron-mobility transistors,” *IEEE Trans. Electron Devices*, vol. 61, no. 8, pp. 2793–2801, Aug. 2014. DOI: 10.1109/TED.2014.2332235

[11] M. Meneghini, N. Ronchi, A. Stocco, G. Meneghesso, U. K. Mishra, Y. Pei, and E. Zanoni, “Investigation of trapping and hot-electron effects in GaN HEMTs by means of a combined electrooptical method,” *IEEE Trans. Electron Devices*, vol. 58, no. 9, pp. 2996–3003, Sep. 2011. DOI: 10.1109/TED.2011.2160547

[12] F. D. Auret, S. A. Goodman, F. K. Koschnick, J.-M. Spaeth, B. Beaumont, and P. Gibart, “Electrical characterization of two deep electron traps introduced in epitaxially grown n-GaN during He-ion irradiation,” *Appl. Phys. Lett.*, vol. 73, no. 25, pp. 3745–3747, 1998. [Online]. Available: http://dx.doi.org/10.1063/1.122881

[13] N. M. Shmidt, D. V. Davydov, V. V. Emtsev, I. L. Krestnikov, A. A. Lebedev, W. V. Lundin, D. S. Poloskin, A. V. Sakharov, A. S. Usikov, and A. V. Osinsky, “Effect of annealing on defects in As-grown and gamma-ray irradiated n-GaN layers,” *Phys. Status solidi B*, vol. 216, no. 1, pp. 533–536, 1999.

[14] M. Meneghini, I. Rossetto, D. Bisi, A. Stocco, A. Chini, A. Pantellini, C. Lanzieri, A. Nanni, G. Meneghesso, and E. Zanoni, “Buffer traps in Fe-doped AlGaN/GaN HEMTs: Investigation of the physical properties based on pulsed and transient measurements,” *IEEE Trans. Electron Devices*, vol. 61, no. 12, pp. 4070–4077, Dec. 2014. DOI: 10.1109/TED.2014.2364855

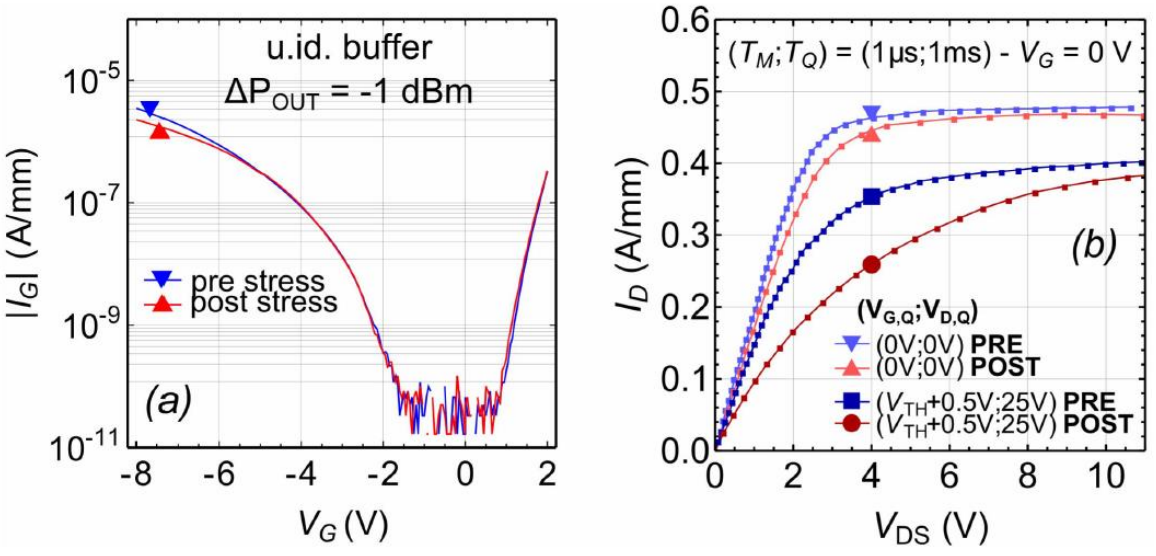

Fig. 1. (a) I_G-V_G characteristics and (b) pulsed I_D vs V_{DS} characteristics acquired prior to and after the stress of a sample with u.i.d. buffer experiencing a ΔP_{OUT} of −1 dBm. No gate-leakage increase and no significant I_{DSS} variation are found. The worsening of the current-collapse is the main evidence of device degradation induced by RF operations.

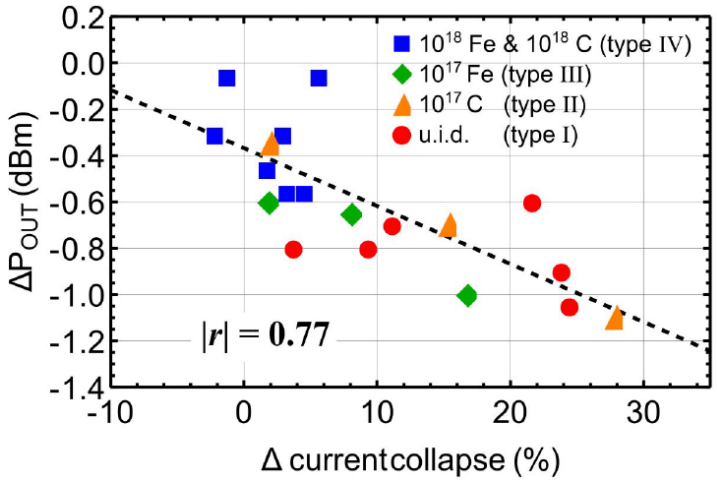

Fig. 2. Good correlation is verified between ΔP_{OUT} and the worsening of current-collapse after RF test.

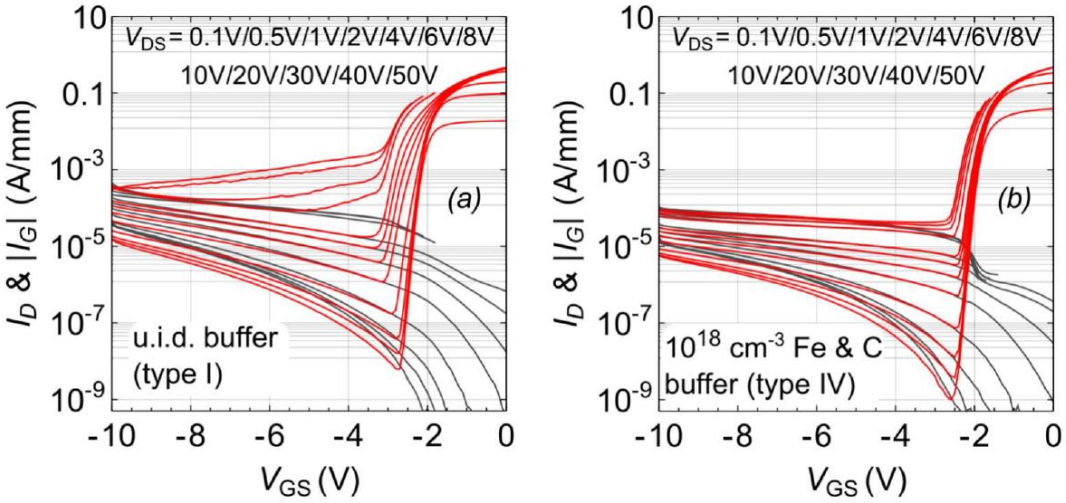

	u.i.d. buffer (type I)	10^{18} Fe & 10^{18} C buffer (type IV)
SS (mV/dec)	91.2	89.2
$\|I_{G,LEAK}\|$ (A/mm)	6.4×10^{-5}	2.4×10^{-5}
DIBL (mV/V)	**69.7**	**22.3**
$I_{D,LEAK}$ (A/mm)	**1.2×10^{-3}**	**3.6×10^{-5}**
$P_{OUT,init}$ (dBm)	29.15	29.10
PAE_{init} (%)	40.4	41.2
ΔP_{OUT} (dBm)	**-1.05**	**-0.55**

Fig. 3. I_D vs V_{GS} and I_G vs V_{GS} characteristics measured at multiple V_{DS} (from 0.1 V to 50 V) for (a) u.i.d. buffer and (b) 10^{18} cm^{-3} Fe- & C-doped buffer HEMTs. Devices with u.i.d. GaN buffer feature higher DIBL, higher $I_{D,LEAK}$, and higher ΔP_{OUT}.

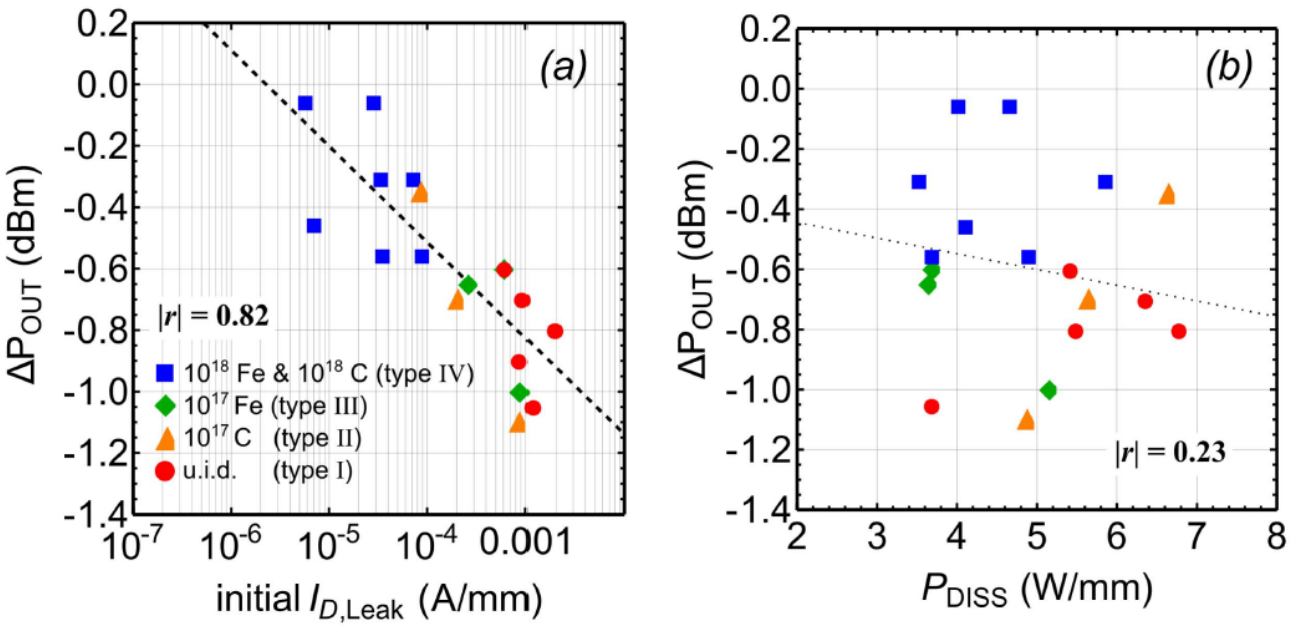

Fig. 4. (a) Good correlation is verified between initial subthreshold source to drain leakage current and RF output power degradation. $I_{D,LEAK}$ is defined at (V_{GS};V_{DS}) = (V_{TH}−1V;40V). (b) No correlation is found between power dissipated during the RF stress and the degradation of the RF output power.

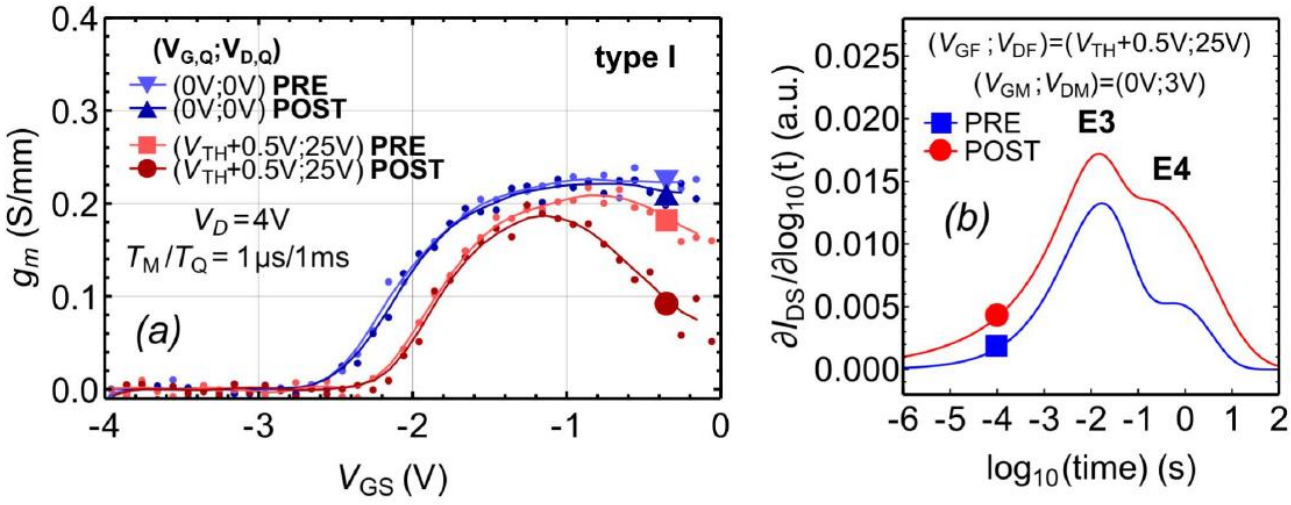

Fig. 5. (a) Pulsed g_m vs V_{GS} characteristics and (b) DCTS performed prior to and after the RF test on a sample with u.i.d. buffer (type I). Stress induces a remarkable gm droop in the hot quiescent bias-point (V_{TH}+0.5V;25V), with the concentration increase of the pre-existing deep levels E3 and E4.

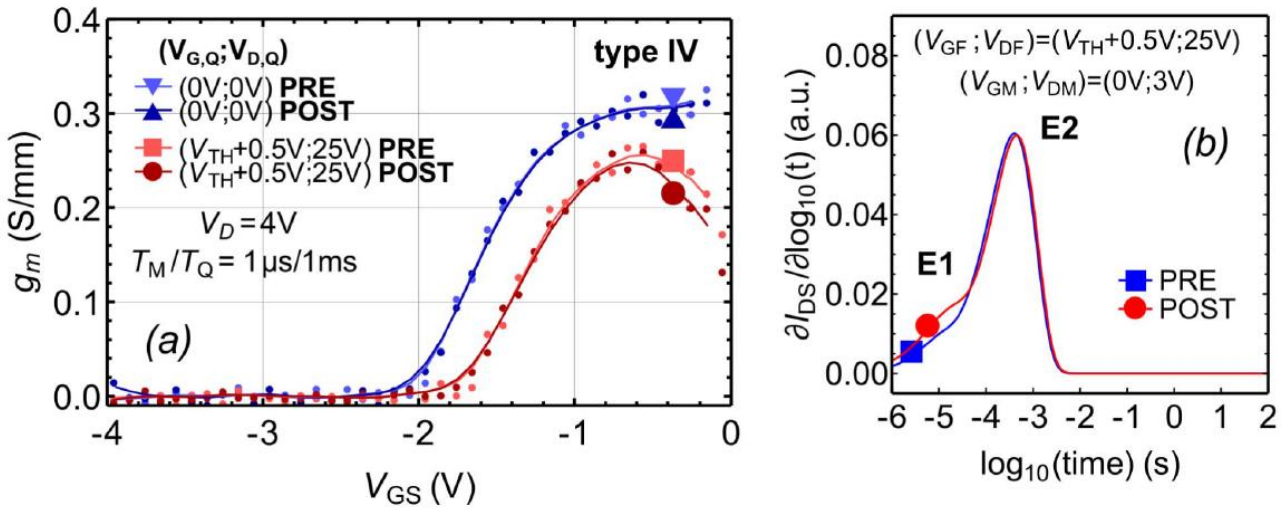

Fig. 6. (a) Pulsed g_m vs V_{GS} characteristics and (b) DCTS performed prior to and after the RF test on a sample with $10^{18}cm^{-3}$ Fe- & C-doped buffer (type IV). After the RF test, only 10% g_m droop is found in the hot quiescent bias-point (V_{TH}+0.5V;25V), with slight increase of pre-existing trap E1, and no relevant increase of trap E2.

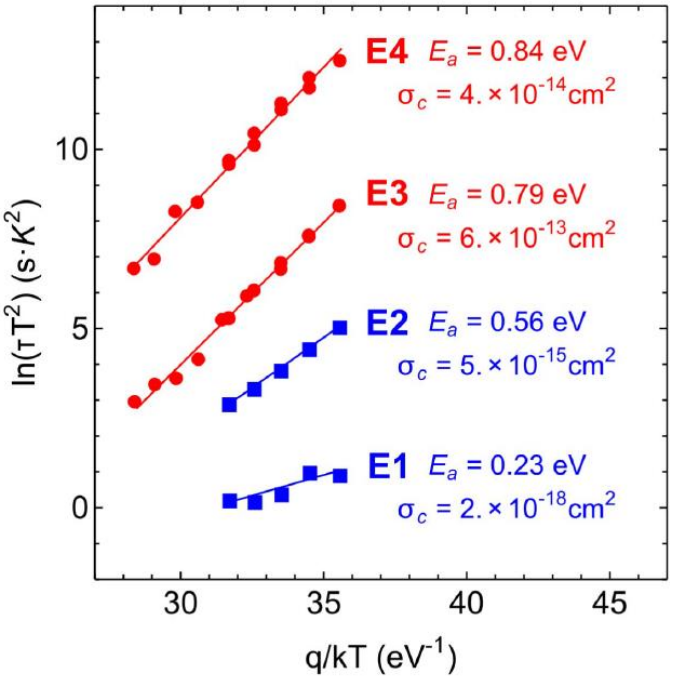

Fig. 7. Arrhenius plot of the deep levels E1, E2, E3, and E4, identified in the tested wafers by means of drain current transient spectroscopy (DCTS).